

Intelligent Controller for Active Walking Guidance of a Robotic Walker

T. V. R. H. Vithanage

Department of Mechanical Engineering

University of Moratuwa

Moratuwa, Sri Lanka

vithanagerhv@gmail.com

N. A. A. N. R. Senaratne

Department of Mechanical Engineering

University of Moratuwa

Moratuwa, Sri Lanka

senaratnenaanr.19@uom.lk

P. D. Welangalle

Department of Mechanical Engineering

University of Moratuwa

Moratuwa, Sri Lanka

welangallepd.19@uom.lk

Y. W. R. Amarasinghe

Department of Mechanical Engineering

University of Moratuwa

Moratuwa, Sri Lanka

ranama@uom.lk

W. A. D. M. Jayathilaka

Department of Mechanical Engineering

University of Moratuwa

Moratuwa, Sri Lanka

dumithj@uom.lk

M. A. M. M. Jayawardane

Department of Obstetrics and Gynaecology

University of Sri Jayawardenepura

Gangodawila, Nugegoda, Sri Lanka

madurammj@yahoo.com

Abstract—Robotic walkers have emerged as an innovative technology in the field of assistive devices, offering enhanced mobility and independence to individuals with physical limitations. In this paper, an intelligent control system for a robotic walker designed to actively guide users using cost-effective force-sensitive resistors has been proposed. The control interface provides a responsive and intuitive user experience. To achieve the desired smoothness and sensitivity of control, a rule-based Fuzzy Inference System (FIS) is implemented. A key safety feature of the walker is its obstacle avoidance system which utilizes haptic feedback to alert users of obstacles in their path. The haptic feedback interface has been developed to indicate both the direction and the proximity of any detected obstacles. The system was tested in a controlled environment with three healthy subjects, and the results demonstrated a satisfactory level of convergence between the user's intended path and the actual path taken by the walker. The haptic feedback system received predominantly positive responses, although some areas for improvement were identified. Future work will focus on enhancing the system's adaptivity to accommodate different pathological conditions.

Index Terms—Robotic Walker, Active Guidance, Fuzzy Control, Rule-based Control

I. INTRODUCTION

The global population is aging rapidly, with the number of individuals aged 60 years or older expected to reach 2 billion by 2050. This demographic shift has led to an increased demand for intelligent assistive devices, particularly robotic walkers, to support the mobility needs of the elderly and individuals with physical impairments. Different approaches have been introduced to support users in walking with the aid of robotic walkers [1].

Recent literature takes a common initiative in utilizing sensor fusion algorithms to perform robust maneuvering of robotic walkers. This can be achieved by detecting user intention using sensor combinations such as an RGB-D camera as in [2], a thermal camera and a 2D LiDAR as in [3], a camera, force sensors, and a laser range finder as in [4], ultrasonic sensors and triaxial load cells as in [5]. To unburden the user of the

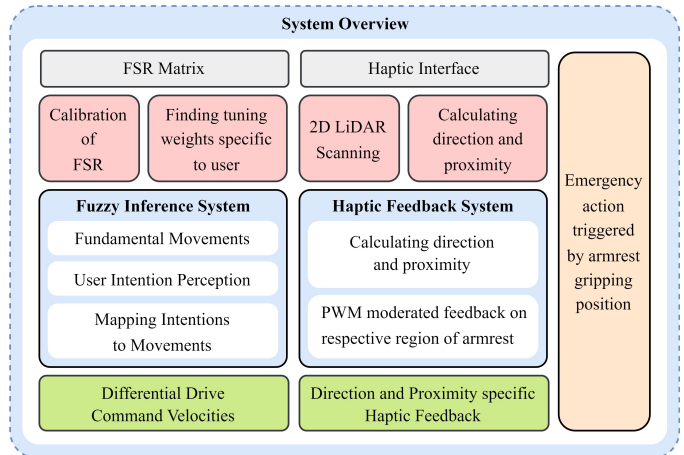


Fig. 1. Overview of the Active Guidance System

requirement to constantly push the walker, methods exist to control the walker without any physical contact between the user and the walker while providing standby support to the user throughout the interaction. This front-following control is made possible mainly by leg tracking using either LiDAR [6], [7], or computer vision [8], [9]. Although the control architecture of such methods allows them to be more precisely controlled, they can be cost-ineffective and computationally more demanding.

Utilizing a joystick control interface [10] is simple and straightforward, but its practical usage can be less intuitive to elderly users with limited fine motor skills. Force sensors that were incorporated into the walker's handlebar frame make up the control interface in [11]. Here to keep the robot's control as simple as possible, a forward push on either of the handlebars causes it to move forward, while a differential push-pull combination causes it to rotate. A tug on either of the handlebars, however, stops the walker. A similar method



Fig. 2. (a) Developed Robotic Walker (b) Overhead view of the armrests laden with force-sensitive resistor matrix and vibrational motors (c) Gripping position of armrests during normal operating conditions (d) Gripping position of armrests for emergency braking action

has been developed using two force-sensing handles in [12].

Alerting the user of obstructions in the surrounding environment is crucial as a sensory aid for frail users with limited spatial awareness. Wearable haptic bracelets that produce vibratory signals to provide haptic guidance have been used in [13] for this purpose. The patient wears a vibrotactile bracelet on each arm to facilitate optimal stimulus separation. When the right bracelet is activated, the user is advised to turn toward the right, whereas when the left bracelet is activated, the user is advised to turn toward the left. When neither band provides haptic feedback, the user is advised to go straight.

The acoustic interface in [14] uses the binaural theory to generate audio signals that guide the user through headphones. For instance, to advise the user to make a turn towards the left, it generates a sound that the user perceives as coming from the left, in other words, a virtual sound source on the left, suggesting a move to be made in that direction.

An overview of the active guidance system proposed in this paper can be visualized using Fig. 1. The implementation employs a force-sensitive resistor (FSR) matrix (Fig. 2 (b)) for receiving force input from the user which after further processing is taken to calculate for velocity output of the driven wheels of the robotic walker (Fig. 2 (a)). The primary contribution lies in the implementation of intelligent control based on fuzzy logic. To notify the user of oncoming obstacles, the active guidance system provides direction-specific haptic feedback, thereby offering comprehensive support.

This paper is structured as follows: Section II details the design and implementation of the intelligent control system. Section III presents experimental results demonstrating the system's effectiveness. Finally, Section IV concludes the paper and discusses future work.

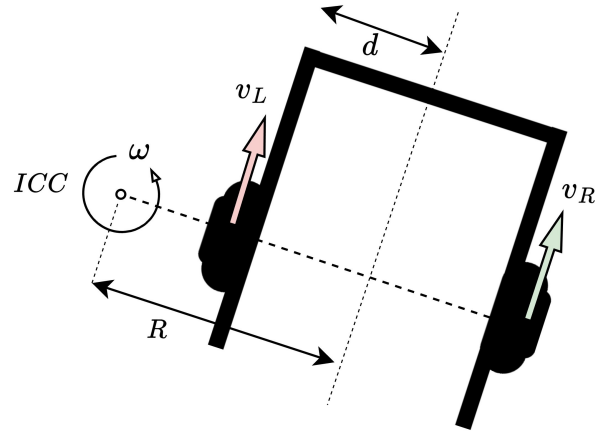


Fig. 3. Kinematics of the differential drive of the robotic walker

II. PROPOSED SYSTEM

A. Robotic Walker Kinematics

The robotic walker prototyped for this research employs a differential drive system with two hub motors (as shown in Fig. 2 (a)) being used to power the platform. It is assumed that both wheels are non-deformable, and the resultant motion is pure rolling without slipping. The plane of each wheel is orthogonal to the ground and the direction of the velocity of the center of mass is orthogonal to the axis connecting the wheels. Passive wheels like casters could be added for further stability and to restrict pitching motion.

A robot's turn is determined by a point along the wheel axis called the Instantaneous Center of Curvature (ICC). The ICC's location affects the type of turn whereas if the ICC is between the wheels, the robot performs a point turn and if the ICC is outside the robot chassis, the robot turns along an arc. The arc's curvature changes with the velocities of the wheels, hence the ICC is only instantaneous. The velocities of the left and right wheels (v_L and v_R) are given by Eq. 1 & 2 where R is the radius of curvature, $2d$ is the distance between the wheel centers, and ω is the rate of rotation. A pictorial depiction of the variables is given in Fig. 3.

$$v_L = \omega \cdot (R - d) \quad (1)$$

$$v_R = \omega \cdot (R + d) \quad (2)$$

These equations can be rearranged to Eq. 3 & 4. From these, some key scenarios can be derived. If $v_R = v_L$, the robot moves in a straight line (forward or backward) as R becomes infinite and ω becomes zero. If $v_R = -v_L$, the robot rotates around its center as R becomes zero. If either v_R or v_L is zero, the robot rotates around the stationary wheel.

$$R = \frac{d \cdot (v_R + v_L)}{v_R - v_L} \quad (3)$$

$$\omega = \frac{v_R - v_L}{2d} \quad (4)$$

Although most prior work implemented fusion approaches of multiple sensor modalities, this paper presents the use of

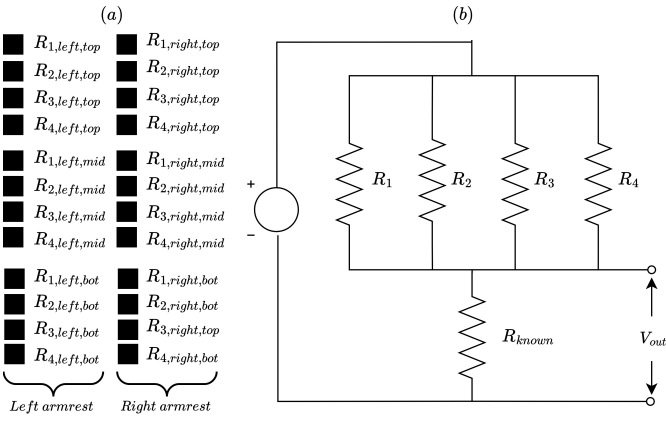


Fig. 4. FIS architectures of (a) standard and (b) hierarchical fuzzy systems

only a single sensor modality for its control interface. FSRs, which have seen growing applications [15] in many domains, are utilized in this application due to cost-effectiveness and their thin and flexible nature allows them to be easily integrated into different form factors.

FSRs are a type of sensor that plays a crucial role in detecting physical pressure, force, or weight. They operate by changing resistance as force is applied to them; the more force you apply, the lower the resistance becomes. This property permits ascertaining the user's force input through the forearms which can then be mapped to a velocity output.

A linear matrix of FSRs provides an easier interfacing setup compared to individual FSRs being put in the same linear arrangement. The arrangement of sensors on the FSR matrix utilized for this control interface is depicted in Fig. 4 (a) with the respective. The branch of four resistors become an equivalent resistance which can be calculated using the Eq. 5. A voltage divider circuit as in Fig. 4 (b) is utilized to obtain the force variation in the form of a voltage variation.

$$R_{eq} = \frac{1}{\frac{1}{R_1} + \frac{1}{R_2} + \frac{1}{R_3} + \frac{1}{R_4}} \quad (5)$$

$f_{left,top}$, $f_{left,mid}$, $f_{left,bottom}$, $f_{right,top}$, $f_{right,mid}$, $f_{right,bottom}$ denote the six corresponding forces recorded at each sensor position. Each of these values corresponds to the equivalent resistances at respective positions and is derived from a unique lookup graph, independently created for each sensor position through a calibration process.

However, with our objective to implement fuzzy inference, it is optimal to minimize parameters in a way the bare minimum is used to understand user intentions. Thus, a preliminary system tuning step is performed to reduce the six sensor locations to four which is consequentially beneficial in making the system adaptive to the user. The reduced system comprises F_{RT} (Right Top), F_{RB} (Right Bottom), F_{LT} (Left Top), and F_{LB} (Left Bottom) as introduced in Eq. 6. For each user a personalized set of tuning weights k_{RT} , k_{RB} , k_{LT} , and k_{LB}

are obtained.

$$\begin{bmatrix} F_{RT} \\ F_{RB} \\ F_{LT} \\ F_{LB} \end{bmatrix} = \begin{bmatrix} k_{RT} \\ k_{RB} \\ k_{LT} \\ k_{LB} \end{bmatrix} \cdot \begin{bmatrix} f_{left,top} \\ f_{left,bottom} \\ f_{right,top} \\ f_{right,bottom} \end{bmatrix} + \begin{bmatrix} 1 - k_{RT} \\ 1 - k_{RB} \\ 1 - k_{LT} \\ 1 - k_{LB} \end{bmatrix} \cdot \begin{bmatrix} f_{left,mid} \\ f_{left,mid} \\ f_{left,mid} \\ f_{left,mid} \end{bmatrix} \quad (6)$$

To perform the tuning step, first-time users are instructed to follow a straight line while using the walker for support. Readings of all sensor locations are recorded, and the tuning weights are then calculated using a linear regression system. The personalized tuning weights are stored in the system along with the user's profile and can be reused. Re-tuning is only necessary if there are significant changes in the user's gait characteristics.

B. Fuzzy Control System

1) *User Intention Perception:* The active guidance system is characterized by a set of seven fundamental movements. These movements have been symbolized for easier comprehension and those are denoted along with the representation of the movements in Fig. 5. Each fuzzy set for force inputs carries two values, High, Low and for each combination of force inputs the desired output in symbolic form is depicted in Table I. In the table, the superscript represents the value of the variable; high or low, while the subscript denotes the position of the sensor.

2) *Mapping intentions to Velocity Commands:* Three outputs characterize the system command: $state$, v_L (left wheel velocity), v_R (right wheel velocity). Each fuzzy set for v_L and v_R encompasses two values: High, Low. The output variable $state$ is a binary variable $state$ that is fuzzified using a singleton membership function, having the values Move, Stop. This $state$ variable simplifies the attainment of the stop condition, preventing first-time users from experiencing oscillation between movements, which could pose a safety concern.

The seven fundamental movements can effectively be mapped to the three outputs as shown in Table II. By combining Table I and Table II, the rule base for the FIS can be created.

3) *FIS Architecture:* The control system serves to translate user intentions into actionable commands for the motor and the Fuzzy Inference System (FIS) that has been developed using MATLAB has been utilized to develop this system. The advantage of fuzzy control systems lies in their adaptability to handling imprecise control inputs, which makes them particularly effective in this application due to the variability of readings of FSRs. Unlike a rule-based system that operates on an if-then-else logic, which can only yield a discrete set of command velocities, fuzzy control systems provide a continuous range of output values which allows for smoother and more nuanced control.

An FIS can be implemented as a tree of smaller interconnected FIS objects rather than as a single monolithic FIS object. This approach, also known as hierarchical fuzzy systems, can help overcome issues related to computational

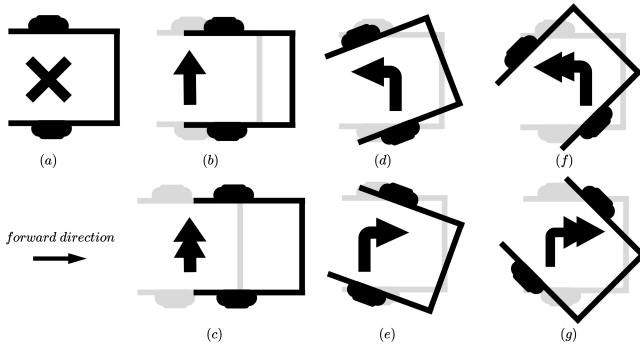


Fig. 5. Fundamental movements of the walker and their symbols (a) Stopped position (b) Forward Slower (c) Forward Faster (d) Wide Left Turn (e) Wide Right Turn (f) Tight Left Turn (g) Tight Right Turn

efficiency, understandability, and tuning of rule and membership function parameters. Both standard and hierarchical (aggregated) fuzzy systems have been implemented in this application. The architectures are denoted along with the type of membership functions in Fig. 6.

The number of membership functions for fuzzification should also be carefully chosen. Although a higher number of linguistic terms can lead to a more accurate controller, it also necessitates more computation, and therefore, a balance between computational demand and accuracy must be struck. The

The specific techniques used for each step of the FIS are given in Table III.

C. Emergency Braking Action

To ensure the safety of the patient two additional FSRs are placed on the curved handlebars of each armrest which will be triggered by even a slight force on either of the sensors and bring the walker to a stop. The placement of the forearm during standard operation and the triggering of the emergency brake are depicted in Fig. 2 (c) and Fig. 2 (d) respectively.

TABLE I
MAPPING USER INPUTS TO THE INTENDED MOVEMENTS OF THE WALKER
(SHADED & UNSHADED CIRCLES INDICATE 'HIGH' AND 'LOW' VALUES AT RESPECTIVE SENSOR POSITIONS)

	$F_{RT}^L F_{RB}^L$	$F_{RT}^L F_{RB}^H$	$F_{RT}^H F_{RB}^L$	$F_{RT}^H F_{RB}^H$
$F_{LT}^L F_{LB}^L$	○○○ X	○○○ ● ↗	○○● ↗	○○● ↗
$F_{LT}^L F_{LB}^H$	○○● ↖	●○○ X	●○○ ↑	●○○ ↗
$F_{LT}^H F_{LB}^L$	●○○ ↖	●○○ ↑	●○○ ↑	●○○ ↑
$F_{LT}^H F_{LB}^H$	●○○ ↖	●○○ ↖	●○○ ↑	●○○ ↑

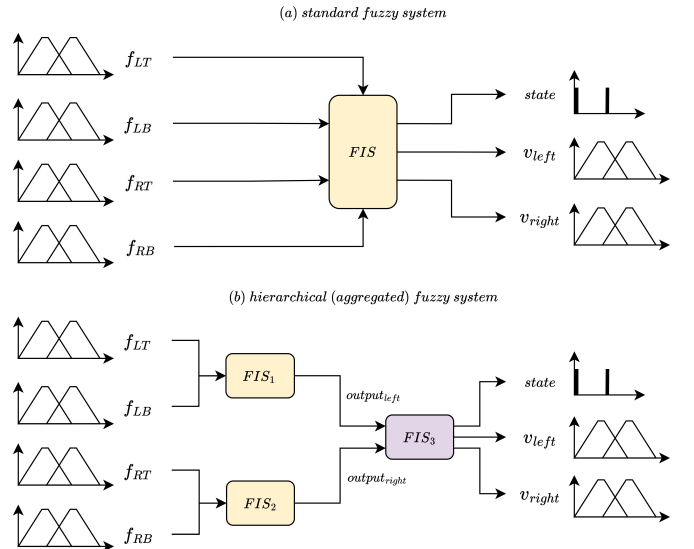


Fig. 6. FIS architectures of (a) standard and (b) hierarchical fuzzy systems

Taking the hands off the armrest will produce the same result, but this additional measure is taken for the user to stop the walker abruptly, even from a leaning position where one or both arms could be rested on the armrests.

D. Obstacle Avoidance with Haptic Feedback

The sensory loss often experienced by frail users may lead to a decreased awareness of ground-level obstacles, which might be aggravated by the walker itself acting as a visual barrier. To address this safety concern, an intuitive obstacle avoidance system is implemented to assist users in maneuvering around objects encountered in their path. A 2D LiDAR sensor, mounted on the front of the walker, is utilized for this purpose which provides an accurate estimation of the direction and proximity of ground-level obstacles encountered from the

TABLE II
MAPPING THE INTENDED MOVEMENTS TO CONTROL OUTPUTS

Movement	X	↑	↑	↖	↖	↗	↗
state	Stop	Move	Move	Move	Stop	Move	Stop
v_L	Low	Low	High	Low	Low	High	High
v_R	Low	Low	High	High	High	Low	Low

TABLE III
METHODS USED UNDER EACH STEP OF FUZZY INFERENCE SYSTEM

Step	Method
Fuzzification	Trapezoid Membership Functions
Rule Evaluation	Mamdani Method
Aggregation	Maximum Aggregation
Defuzzification	Centroid Method

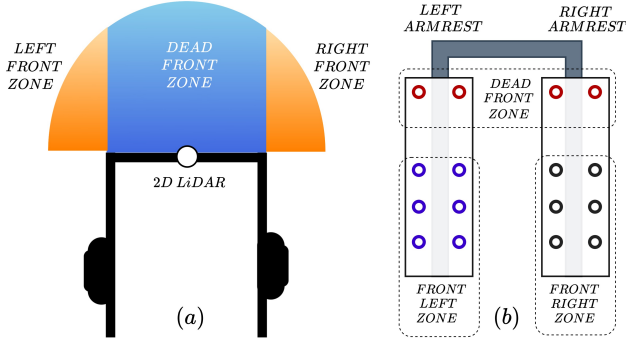


Fig. 7. (a) Utilizable scan range and segmented regions of detection (b) Corresponding feedback zones on armrest

front. Given that the walker's differential drive system does not permit lateral movement, the detection of obstacles in the front is deemed sufficient for safe and efficient navigation.

The mounting location of the LiDAR sensor and its detection zone is depicted in Fig. 7 (a). To ensure the intuitiveness of the feedback the detection zone is only segmented into three regions, named Dead Front, Left Front, and Right Front. To provide positional feedback of detected obstacles a set of micro vibrational motors are arranged on the top of each armrest. Detection in each region by the 2D LiDAR is mapped to the respective region of the armrest for haptic feedback. The mounting locations of the vibrational motors and the respective regions are shown in Fig. 7 (b).

Regional segmentation provides the direction of the obstacle, but the system can be improved to provide the distance to the obstacle as well, by utilizing the frequency of the motor vibration to provide proximity information. Pulse width modulation (PWM) is used to moderate the frequency inversely proportional to the distance to the obstacle. Vibrations are initiated only after the distance falls below a certain threshold. The threshold can be manually adjusted suiting to the environment and operational speeds of the walker. To minimize the aftereffect problem the maximum vibration frequency was kept below 280 Hz [R21], to prevent the user from experiencing continuous stimuli that make the stimulation insensitive altogether.

E. Experimental Setup

A controlled environment was set up with various obstacles placed at different locations. to mimic real-world conditions. Three healthy male subjects, A, B & C, in the age range of 24 ± 2 were instructed to walk with the support of the walker. Input data; force inputs f_{RT} , f_{RB} , f_{LT} , f_{LB} and output data; state, v_L , v_R are separately recorded.

To assess the robustness under varying control velocities, three subjects were asked to walk from a starting point to an endpoint while navigating around obstacles, roughly in the shape of a 'S' letter. Each subject walked at a different pace: Subject A walked at the average pace of a healthy older adult, Subject B walked at a pace slower than the average, and

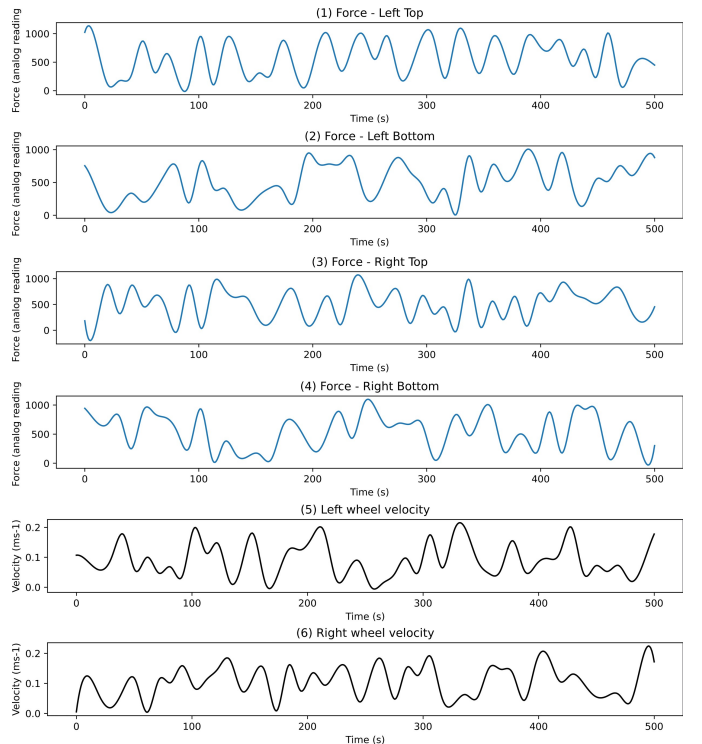


Fig. 8. Recorded data for subject A (1)-(4) Input forces (5),(6) Output command velocities

Subject C walked at a pace faster than the average. For safety reasons, the maximum velocity of the walker was set at 0.4 m/s. As an additional step, all participants followed the same path using the walker in an unpowered state, to facilitate a comparative analysis.

Responses to a questionnaire regarding the intuitiveness, learning curve of the active guidance system, and the reliability, and obtrusiveness of the haptic feedback system were collected from each participant.

III. RESULTS

Fig. 8 indicates the recorded data for subject A, where the former shows the input forces and the latter shows the output command velocities. Fig. 9 plots the simulated paths obtained from input data and output data separately along with the recorded path when using the walker in an unpowered state. The deviations between the simulated output path and path under the unpowered-walker condition for all three subjects are shown in Fig. 10.

IV. CONCLUSION

A satisfactory level of convergence between the intended and actual path can be observed from the plots. Although not significant, changing velocities have affected the path convergence. As speeds increase, the smoothness of turns diminishes a finding that was also noted in the questionnaire responses. During tighter turns, users need to exercise more caution in applying forces, which may impose an additional cognitive load on older users. All subjects agreed on the

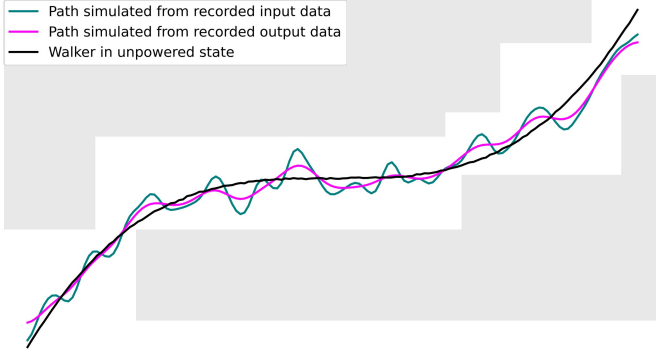


Fig. 9. Simulated paths from recorded input data and output data and the path followed with the walker in unpowered state

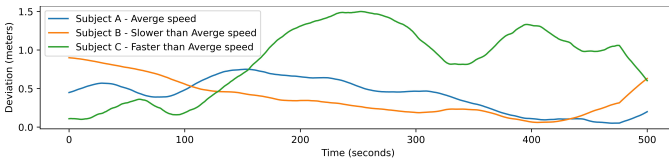


Fig. 10. Deviations between the simulated output path and the path followed with the walker in unpowered state

learning curve required to gain confidence in the system's responses to user inputs.

The majority of the responses towards the haptic feedback system were positive although there were several remarks concerning false detections. An object that the 2D LiDAR initially detects as present within the detection zone might be a false indication of an object located further away. In such cases, the immediate activation of the haptic system could startle the user and undermine the system's reliability. One potential solution to this issue is to introduce a delay period after the object's initial detection. This delay would allow for more accurate confirmation of the object's presence before activating the haptic feedback. Another alternative could be to enhance the system with a hybrid solution that combines the LiDAR sensor with a camera running an object detection algorithm. This approach could potentially improve the accuracy of object detection and reduce the occurrence of false positives.

In conclusion, this paper presented an intelligent control system for a robotic walker, designed to actively guide users using cost-effective force-sensitive resistors. The system demonstrated satisfactory convergence between the user's intended path and the actual path taken by the walker. The haptic-feedback-based obstacle avoidance system, a key safety feature, received predominantly positive responses, although some areas for improvement were identified.

For future work, a force-sensitive resistor matrix with a denser packing of resistors could be employed to provide higher resolution and more coverage of the forearms enabling more detailed and precise measurements. Reinforcement Learning could be utilized to learn the tuning weights rather than a regression method. Additionally, further experi-

mentation is needed to establish whether a data-driven system such as an Adaptive-Neuro-Fuzzy Inference System (ANFIS) could outperform a FIS system for this application.

REFERENCES

- [1] S. D. Sierra M., D. E. Garcia A., S. Otálora, M. C. Arias-Castro, A. Gómez-Rodas, M. Múnera, and C. A. Cifuentes, "Assessment of a robotic walker in older adults with parkinson's disease in daily living activities," *Frontiers in NeuroRobotics*, vol. 15, 2021. [Online]. Available: <https://www.frontiersin.org/articles/10.3389/fnbot.2021.742281>
- [2] M. Palermo, S. Moccia, L. Migliorelli, E. Frontoni, and C. P. Santos, "Real-time human pose estimation on a smart walker using convolutional neural networks," *Expert Systems with Applications*, vol. 184, p. 115498, 2021. [Online]. Available: <https://www.sciencedirect.com/science/article/pii/S0957417421009088>
- [3] Z. Chongyu, G. Wenzhi, W. Rongwei, Z. Wang, and C. Wu, "Deep learning-driven front-following within close proximity: a hands-free control model on a smart walker," in *2022 International Conference on Robotics and Automation (ICRA)*, 2022, pp. 812–818.
- [4] C. Molano, L.-P. Chen, and L.-C. Fu, "Robotic walker with high maneuverability through deep learning for sensor fusion," in *2019 IEEE International Conference on Systems, Man and Cybernetics (SMC)*, 2019, pp. 1024–1029.
- [5] S. D. Sierra M., M. Garzón, M. Múnera, and C. A. Cifuentes, "Human-robot-environment interaction interface for smart walker assisted gait: Agora walker," *Sensors*, vol. 19, no. 13, 2019. [Online]. Available: <https://www.mdpi.com/1424-8220/19/13/2897>
- [6] W. Chung, H. Kim, Y. Yoo, C.-B. Moon, and J. Park, "The detection and following of human legs through inductive approaches for a mobile robot with a single laser range finder," *IEEE Transactions on Industrial Electronics*, vol. 59, no. 8, pp. 3156–3166, 2012.
- [7] Q. Xiao, F. Sun, R. Ge, K. Chen, and B. Wang, "Human tracking and following of mobile robot with a laser scanner," in *2017 2nd International Conference on Advanced Robotics and Mechatronics (ICARM)*, 2017, pp. 675–680.
- [8] M. Gupta, S. Kumar, L. Behera, and V. K. Subramanian, "A novel vision-based tracking algorithm for a human-following mobile robot," *IEEE Transactions on Systems, Man, and Cybernetics: Systems*, vol. 47, no. 7, pp. 1415–1427, 2017.
- [9] B. X. Chen, R. Sahdev, and J. K. Tsotsos, "Person following robot using selected online ada-boosting with stereo camera," in *2017 14th Conference on Computer and Robot Vision (CRV)*, 2017, pp. 48–55.
- [10] M. M. Martins, A. Frizera-Neto, E. Urendes, C. dos Santos, R. Ceres, and T. Bastos-Filho, "A novel human-machine interface for guiding: The neoasas smart walker," in *2012 ISSNIP Biosignals and Biorobotics Conference: Biosignals and Robotics for Better and Safer Living (BRC)*, 2012, pp. 1–7.
- [11] A. Morris, R. Donamukkala, A. Kapuria, A. Steinfeld, J. Matthews, J. Dunbar-Jacob, and S. Thrun, "A robotic walker that provides guidance," in *2003 IEEE International Conference on Robotics and Automation (Cat. No.03CH37422)*, vol. 1, 2003, pp. 25–30 vol.1.
- [12] C.-K. Lu, Y.-C. Huang, and C.-J. Lee, "Adaptive guidance system design for the assistive robotic walker," *Neurocomputing*, vol. 170, pp. 152–160, 2015, advances on Biological Rhythmic Pattern Generation: Experiments, Algorithms and Applications Selected Papers from the 2013 International Conference on Intelligence Science and Big Data Engineering (IScIDE 2013) Computational Energy Management in Smart Grids. [Online]. Available: <https://www.sciencedirect.com/science/article/pii/S0925231215008826>
- [13] B. Graf, "An adaptive guidance system for robotic walking aids," *Journal of Computing and Information Technology*, vol. 17, no. 1, pp. 109–120, 2009.
- [14] F. Moro, A. De Angeli, D. Fontanelli, R. Passerone, D. Prattichizzo, L. Rizzon, S. Scheggi, S. Targher, and L. Palopoli, "Sensory stimulation for human guidance in robot walkers: A comparison between haptic and acoustic solutions," in *2016 IEEE International Smart Cities Conference (ISC2)*, 2016, pp. 1–6.
- [15] A. S. Sadun, J. Jalani, and J. A. Sukor, "Force Sensing Resistor (FSR): a brief overview and the low-cost sensor for active compliance control," in *First International Workshop on Pattern Recognition*, ser. Society of Photo-Optical Instrumentation Engineers (SPIE) Conference Series, X. Jiang, G. Chen, G. Capi, and C. Ishll, Eds., vol. 10011, Jul. 2016, p. 1001112.